JSR Publications

Available Online

J. Sci. Res. **17** (1), 247-257 (2025)

JOURNAL OF SCIENTIFIC RESEARCH

www.banglajol.info/index.php/JSR

Synthesis and Characterization of Binary (Ni:Cu) Metal Oxide Thin Film via Sol-Gel Spin Coating Method for Electrochemical Capacitor Application

S. C. Gavandi[1*], S. S. Mahajan[1], D. S. Sutrave[2]

[1]Jaysingpur College, Jaysingpur, Taluka-Shirol, Shivaji University, District-Kolhapur 416101(MS) India

[2]D.B.F. Dayanand College of Arts and Science, Dist. Solapur, Maharashtra, India

Received 4 April 2024, accepted in final revised form 20 August 2024

Abstract

In the present work, binary (Ni:Cu) metal oxide electrode material has been synthesized using the sol-gel spin coating technique. NiCuO exhibits cubic crystal structure and porous, rough surface morphology. The binary nickel copper metal oxide electrode shows a maximum specific capacitance of 781 F/g measured in KOH electrolyte at a scan rate of 5 mVs^{-1}. From the discharging curve, a maximum specific capacitance of 248 F/g is obtained at a current density of 1 mA/cm^2. Additionally, the NiCuO electrode has a power density of 206 KW/kg and an energy density of 21 Wh/kg at 1 mA/cm^2 with 73 % efficiency. Because of its hydrophilicity and porous agglomerated surface, binary (Ni:Cu) metal oxide is a suitable electrode material for Supercapacitor application.

Keywords: (Ni:Cu) oxide; Sol-gel; Aqueous electrolyte; Supercapacitor; Thin film.

doi: https://dx.doi.org/10.3329/jsr.v17i1.72486 J. Sci. Res. **17** (1), 247-257 (2025)

1. Introduction

Because of energy crisis as well as the problem of the deterioration of the environment is increasingly serious, people need sustainable and potent energy storage devices [1,2]. Electrochemical capacitors also called super capacitors are one of the most important energy storage devices. They have gained considerable attention because of their short charging time, long cycle life, high power as well as high energy densities [3-7]. Based on charge-storage mechanisms, electrochemical capacitors (ECs) are categorized into two fundamental types, electrochemical double-layer capacitor (EDLC) and pseudocapacitor (PSC) [8]. During the electrostatic (non-faradic) charge storage process in EDLC, ions/electrons accumulate on the electrode surface. Electrochemical (faradic) charge storage in PSCs occurs at the surface and near the surface of the electrode material. Carbon and its derivatives are suitable as EDLC electrodes, while transition metal oxides (TMOs) and conducting polymers are appropriate for use as PSCs electrodes [9]. The high specific capacitance of TMOs compared to that of carbon-based materials makes them more suitable for SC applications because of which they are being widely studied. Amid transition metal

* *Corresponding author*: savitagavandi@gmail.com

oxides, Nickel Oxide is one of the good materials for Pseudocapacitor performance. On account of their outstanding electrochemical activity, nickel compounds have been used extensively as electrode materials [10].

Along with this, binary transition metal oxides have also attracted a wide range of concerns as supercapacitor electrode materials because of their high stability and superb electronic conductivity [11]. Nickel cobalt oxide [12], cobalt copper oxide [13,14], and copper manganese oxide [15] are the best examples to show awesome electrochemical performance against corresponding single metal oxide.

Out of these electrode materials candidates, binary nickel-copper metal oxide has enhanced interest due to several fascinating advantages. More precisely, copper is considered the best candidate for electrode materials because of its good conductivity, low-cost abundant resources, green environmental protection, and high chemical stability [16].

In the current work, we examined the electrochemical performance of binary Nickel Copper metal oxide electrodes using 0.1 M KOH electrolyte solution. The NiCuO electrode is prepared by a simple Sol-gel spin coating method which is convenient for obtaining porous structured electrodes. The electrochemical behavior of the electrochemical capacitor is analyzed by cyclic Voltametry (CV), Galvanostatic charge-discharge, and Electrochemical Impedance Spectroscopy (EIS) techniques. The NiCuO electrode shows a maximum specific capacitance of 781 F/g measured in KOH electrolyte at a scan rate of 5 mVs^{-1} with 206 KW/Kg and energy density of 21 Wh/kg at $1mA/cm^2$. The surface area of the as-deposited binary (Ni : Cu) metal oxide is obtained to be 5.688 $m^2\ g^{-1}$ from the BET plot.

2. Experimental

2.1. *Materials*

Reagents like nickel chloride ($NiCl_2{\cdot}6H_2O$), cupric chloride ($CuCl_2{\cdot}2H_2O$), and ethanol (AR grade) were brought from Thomas Baker, India, without including any chemical treatment.

2.2. *Preparation of binary (Ni : Cu) metal oxide thin film*

Binary (Ni:Cu) metal oxide thin films were deposited on a stainless steel (SS) substrate via the Sol-gel method followed by annealing. First of all, the solution was prepared by taking 0.0125 M Nickel chloride ($NiCl_2{\cdot}6H_2O$) and 0.2 M cupric chloride ($CuCl_2{\cdot}2H_2O$) precursors. Initially, stainless steel substrates were polished with the help of zero-grade polish paper then the substrates were cleaned using detergent, washed thoroughly with double distilled water, then rinsed with acetone, and dried completely. The solution was prepared with a percentage of Cu at 50 %. Ethanol was then added to the solution for the gel formation and stirred for 6 h on a magnetic stirrer at a temperature of 60 °C. For the sake of the formation of gel, the solution was kept aside for 24 h. A clear and viscous solution was formed after aging. The obtained solution was light blue in color. Then this

solution was used for deposition on the stainless steel substrate via the spin coating deposition technique. Then obtained thin films were annealed at 400 °C.

2.3. *Characterizations*

The structural analysis was carried out using X-ray Diffractometry (XRD) with Cu-Kα radiation (λ = 1.54 Å). JEOL JSM-IT200 scanning electron microscope (SEM) instrument is used for surface morphological analysis as well as for compositional analysis. Bruker Alpha spectrophotometer (375 to 7500 cm^{-1}) is used for the FT-IR. The electrochemical analysis of the as-deposited binary (N i: Cu) metal oxide thin film electrode was carried out using the EIS technique by Zive MP1 Multichannel instrument. Synthesized NiCuO electrode is utilized as a working electrode, platinum as a counter electrode, and Hg/HgO (Mercury/Mercury Oxide Electrode) as a reference electrode. BET analysis was carried out using the BET surface area analyzer instrument.

3. Results and Discussion

3.1. *XRD analysis*

The structural studies of as-deposited nickel copper film were carried out using X-ray Diffractometry. The XRD result of binary (Ni:Cu) metal oxide thin films annealed at 400°C is shown in Fig. 1. The samples are crystalline. XRD patterns were obtained with source CuKα (λ = 1.54 Å), 2θ angle varied from 20° to 90°. The XRD pattern implies that deposited films are crystalline with a cubic structure. XRD pattern indicated the peaks of Nickel oxide as well as copper oxide but a dominating peak is observed for Copper oxide [17].

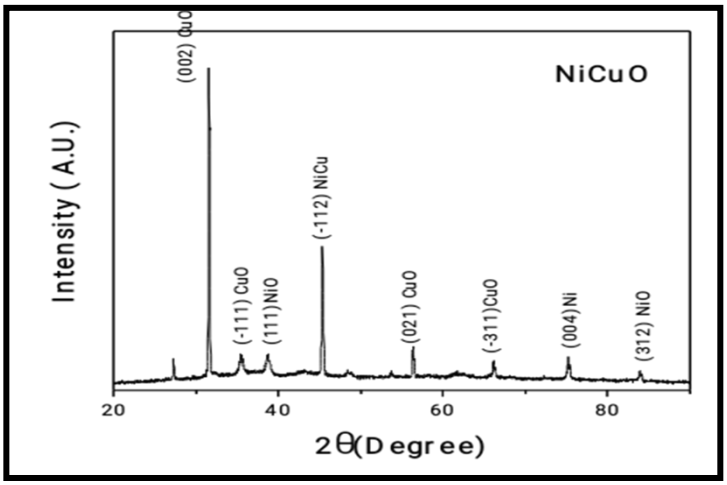

Fig. 1. X-ray Diffraction pattern of binary metal (Ni:Cu) oxide thin film.

3.2. *SEM analysis*

The SEM micrographs exhibited the formation of a thin film and it is well adherent to the substrate. These images of binary metal (Ni:Cu) oxide with different magnifications are shown in Fig. 2. SEM images contain several irregularly arranged agglomerates which form a rough surface with porous morphology. The porosity results in the possibility of better electrochemical supercapacitor behavior of binary (Ni:Cu) metal oxide thin film [18].

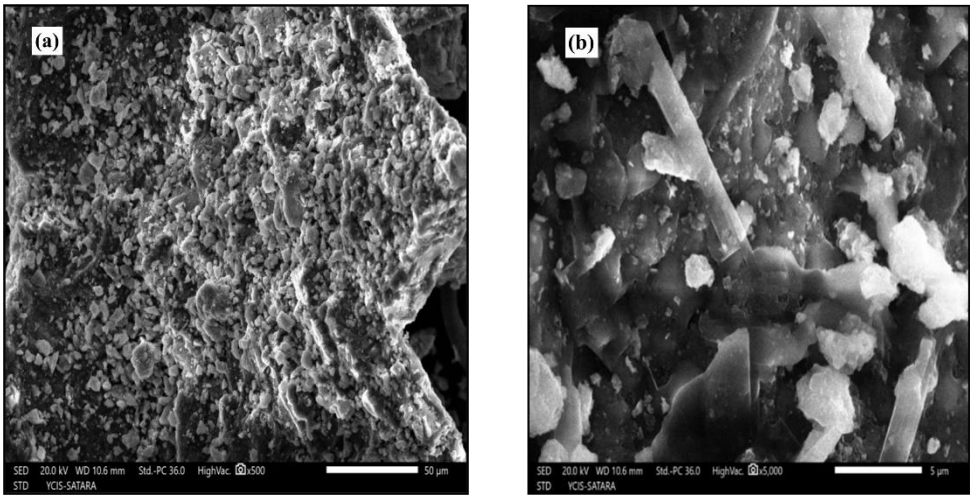

Fig. 2. SEM images of binary metal (Ni:Cu) oxide thin film at (a) X500 magnification and (b) X5000 magnification.

3.3. *EDAX analysis*

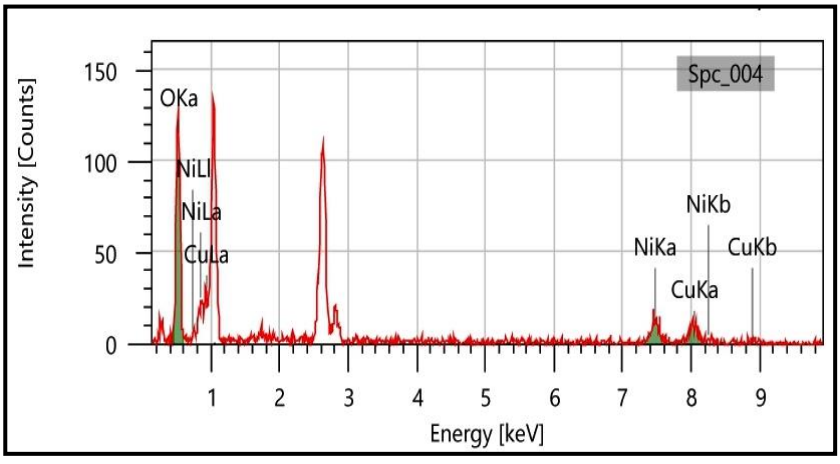

Fig. 3. Energy-dispersive X-ray analysis of binary metal (Ni:Cu) oxide thin film.

EDAX spectrum was shown in Fig. 3 to explore the elemental composition of the as-prepared material surface. It shows the formation of binary (Ni:Cu) metal oxide on the substrate. In the EDAX measured result, nickel, copper, and oxygen were observed which gave evidence for the formation of binary (Ni:Cu) metal oxide on the substrate.

3.4. *FT-IR analysis*

Fourier Transform Infrared Spectroscopy (FT-IR) gives an idea regarding functional groups of compounds. Fig. 4. shows the FT-IR spectrum of binary (Ni:Cu) metal oxide recorded during 400 to 4000 cm^{-1}. The dominant peak at 495 cm^{-1} corresponds current absorption bond. The peak observed at 1048, 1222, 1384, and 1631 cm^{-1} corresponds to –COO carboxylic acid, C=O stretching While the peaks at 2852, 2878, 2923 cm^{-1} corresponds to C–H bonding. The wide band around 3434 cm^{-1} belongs to O–H stretching vibrations indicating hydrous in nature [19].

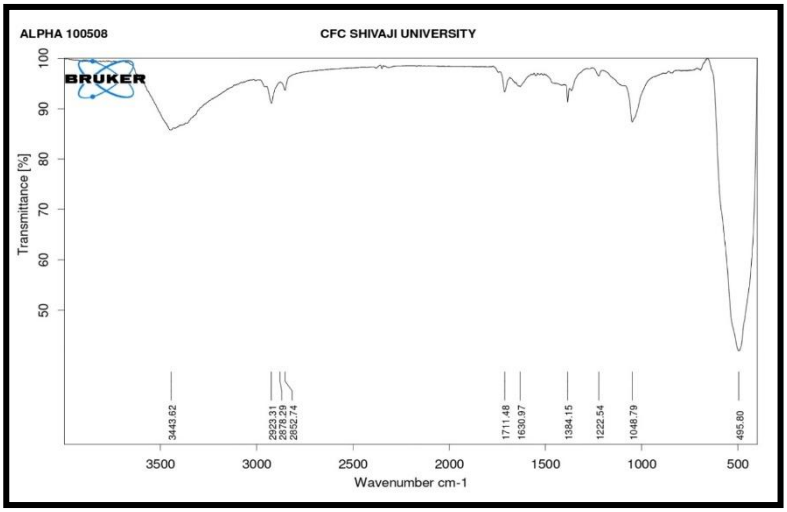

Fig. 4. Fourier Transform Infrared Spectroscopy graph of binary metal (Ni:Cu) oxide thin film.

3.5. *Angle of contact analysis*

A surface Wettability test was performed to know the interaction between the liquid and NiCuO thin film. High wettability leads to a small contact angle (θ) and the surface is hydrophilic. On the contrary, Low wettability leads to a large contact angle (θ) and the surface is hydrophobic. A contact angle of 0° corresponds to complete wetting and a contact angle of 180° gives rise to complete non-wetting. The super hydrophilic surfaces are dominant for supercapacitor application. The contact angle of the NiCuO electrode with water is shown in Fig. 5. The contact angle is observed to be 78° which is hydrophilic in nature [20].

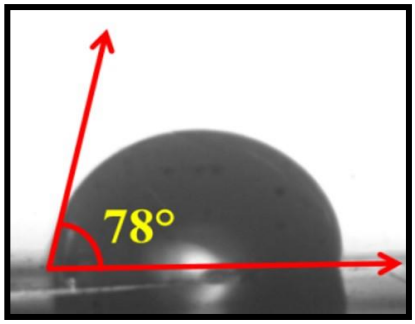

Fig. 5. Surface wettability test of binary metal (Ni:Cu) oxide thin film.

3.6. *Electrochemical analysis by cyclic voltammetry*

The CV is an important technique in electrochemistry which provides qualitative information about the electrochemical process, whether the process is Faradic or non-Faradic, that takes place in the material. The electrochemical analysis of binary metal (Ni:Cu) oxide thin film was done with cyclic Voltammetry (CV) measurements and was subjected at various scan rates from 5 mV/s to 100 mV/ s in 0.1 M KOH electrolyte with a potential window of 0 V to 0.5 V. During the different scan rate, it was observed that the current under the curve gradually increased with scan rate. From this, we can conclude that Voltammetric current is directly proportional to the scan rates of CV and is a good sign of supercapacitive behavior [21].

To calculate the specific capacitance (SC) of the electrode from the CV curves following formula was used.

$$SC = \frac{c}{m} = \frac{\int_{v1}^{v2} I\, dV}{m(V)\frac{dV}{dt}} \quad (1)$$

Where *m* is the mass of active material, V1 and V2 are the potential limits, $\frac{dV}{dt}$ is the scan rate potential.

Fig. 6 shows cyclic voltammograms with a potential window of 0 V to 0.5 V at various scan rates 5, 20, 50, 80, and 100 mV s^{-1}. From CV analysis, the electrode exhibited a maximum specific capacitance of 781 F/g at 5 mVs^{-1} scan rate. The obtained results of the NiCuO electrode with various scan rates are given in Table 1. As the current under the curve slowly increased with scan rate, we conclude that the Voltammetric current is directly proportional to scan rate and this is a good indication of supercapacitive behavior.

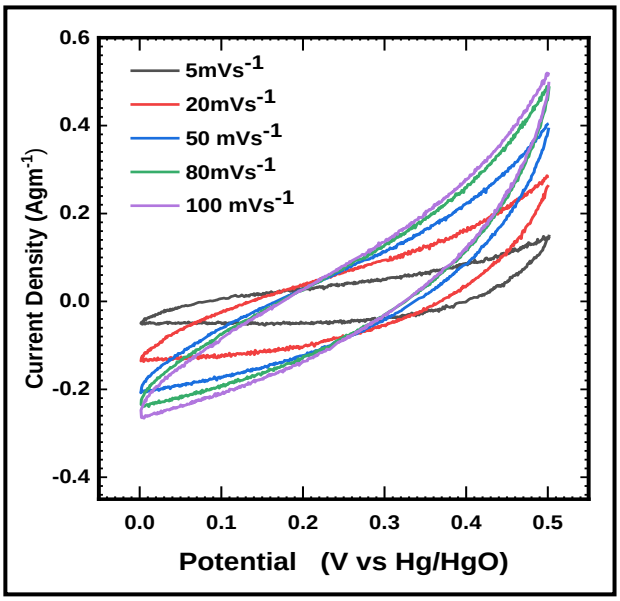

Fig. 6. Cyclic voltammograms curves of NiCuO thin film electrode in 0.1 M KOH electrolyte.

Table 1. Specific capacitance at various scan rates of NiCuO thin film electrode in 0.1 M KOH electrolyte.

Scan rate (mV/s)	Specific capacitance (F/g)
5	781.1
20	397.8
50	221.0
80	160.0
100	137.0

3.7. *Galvanostatic charge-discharge*

Galvanostatic charge-discharge curves at various current densities of binary metal (Ni: Cu) oxide are shown in Fig. 7. The specific capacitance, can also calculated from charging/discharging curves according to the equation

$$Cs = \frac{I \,.\, t}{m \,.\, \Delta V} \qquad (2)$$

Where 'I' is the applied charging/discharging current, t is the discharge time, m indicates the mass of active electrode material and ΔV is the potential range of the scanning segment [22]. The specific capacitance is calculated according to the discharging curve using the above formula. A specific capacitance of 248 F/g is obtained at a current density of 1 mA/cm^2.

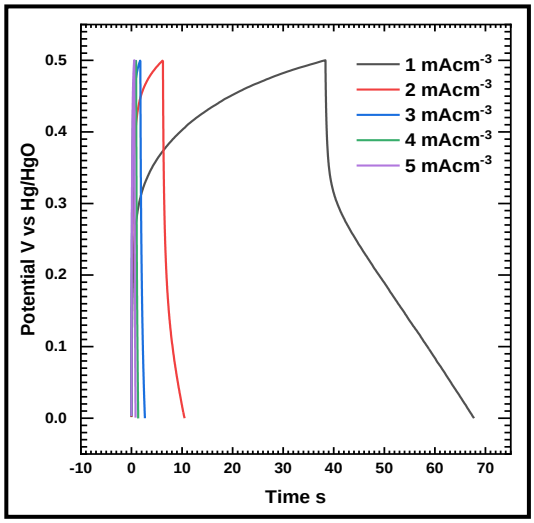

Fig. 7. Charge discharge curves of NiCuO electrode in 0.1 M electrolyte.

The electrical parameters like specific power (SP) and specific energy (SE) were calculated using the following relations [23].

$$SP = \frac{I \times V}{m} \tag{3}$$

$$SE = \frac{I \times t \times V}{m} \tag{4}$$

Where, SP specific power is in KW/Kg and SE is specific energy in Wh/kg. The above expressions indicate discharge current (I) in amperes, voltage range (V) in volts, mass of electroactive material (m) in kilograms, and discharge time in seconds. We obtained a power density of 206 KW/kg and an energy density of 21 Wh/kg at 1 mA/cm^2 respectively. The columbic efficiency is calculated using the following relation [24].

$$\eta = \frac{\mathrm{tD}}{tC} \times 100 \tag{5}$$

Where t_C and t_D denote the time of charging and discharging respectively. The calculated columbic efficiency is 73 %.

3.8. *Electrochemical impedance spectra analysis*

The charge transfer study of binary (Ni:Cu) metal oxide thin film electrodes was carried out in the frequency range of 0.01 Hz to 100 kHz. The equivalent circuit we chose to fit the measured EIS data is shown in Fig. 8a the fitted result (red dots) shows a quite good match with the measured result (black dots). In this circuit, R_s represents equivalent series resistance, R_1 represents electrolyte resistance, R_2 represents charge transfer resistance and W is the Warburg diffusion resistance [25]. Fig. 8b obviously represents three variation ranges including a partial semi-circle part, a slope with 45°, and a slope with an angle of

more than 70°. It is well known that a larger semicircle means a larger charge transfer resistance; the slope with 45° indicates the Warburg resistance caused by electrolytic ions diffusion and a steeper slope signifies a lower ion-diffusion rate [26].

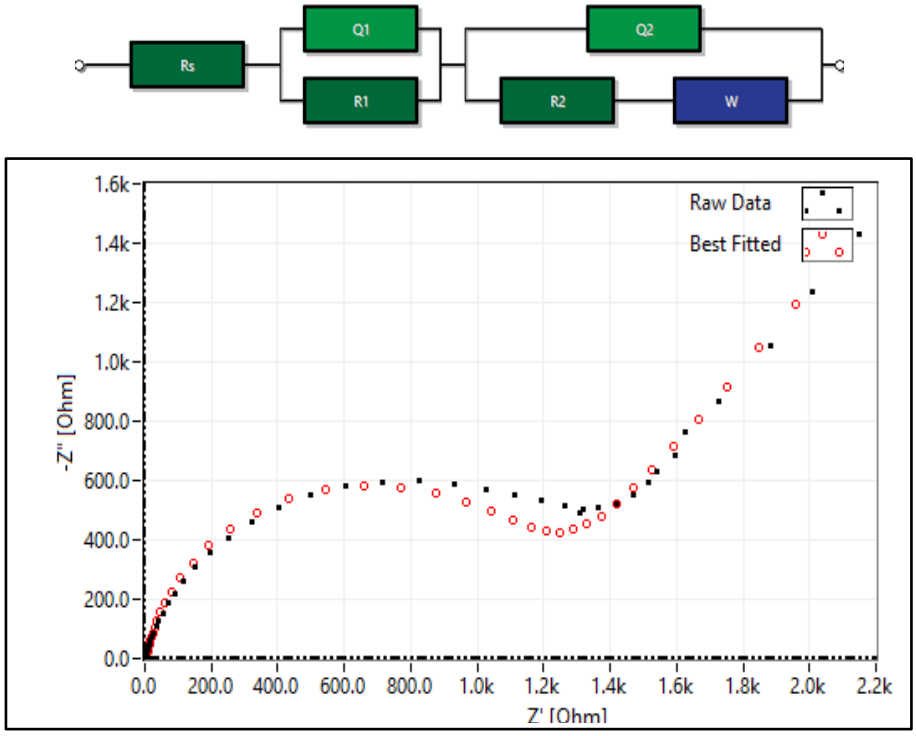

Fig. 8. Electrochemical impedance spectra of NiCuO electrode in 0.1 M electrolyte (a) Equivalent circuit (b) Nyquist plots at frequencies between 100 kHz and 0.01 Hz.

3.9. *BET analysis*

To confirm the specific area and pore size of the NiCuO samples, the product was tested by BET nitrogen adsorption-desorption measurements. The specific area of the as-deposited samples was estimated using the Brunauer-Emmett-Teller (BET) equation based on the nitrogen adsorption isotherm [27]. The BET plot of the as-deposited binary (Ni:Cu) metal oxide thin film is shown in Fig. 9. The Brunauer-Emmett-Teller (BET) surface area of the sample is calculated to be 5.688 $m^2 g^{-1}$. The mean pore diameter of 33.631 nm is obtained.

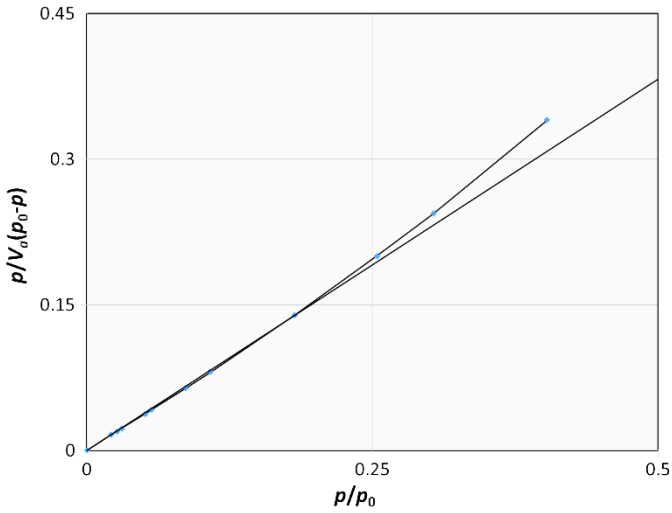

Fig. 9. Brunauer-Emmett-Teller plot of binary (Ni:Cu) metal oxide thin film.

4. Conclusion

It is concluded that binary (Ni:Cu) metal oxide thin film has been successfully deposited on SS substrate and employed as a supercapacitor. The presence of characteristic bonds of nickel-copper oxide was verified by FT-IR studies. A rough surface having a porous morphology offers more active sites for electrochemical reactions. NiCuO electrode exhibits the maximum specific capacitance obtained is 781 F/g at 5 mV^{-1} scan rate. From GCD a high specific capacitance of 248 F/g is obtained at a current density of 1 mA/cm^2. The power density (P) and energy density (E) were 206 KW/kg, 21 Wh/kg at 1mA/cm^2 and efficiency is 73 %. From BET analysis the surface area of the sample is calculated to be 5.688 $m^2\ g^{-1}$. This study corroborates that nickel copper oxide is a promising material as an electrochemical capacitor electrode.

Acknowledgments

The author S. C. Gavandi thanks the SAIF-CFC-DST centre, Shivaji University, Kolhapur for providing a material characterization facility. Additionally, the author would like to thank Research and Development, Y. C. Institute of Science, Satara for providing a material characterization facility.

References

1. L. Liang, H. Liu, and W. Yang. J. Alloys Comp. **559**, 168 (2013). https://doi.org/10.1016/j.jallcom.2013.01.111
2. A. S. Arico, P. Bruce, B. Scrosati, and J. -M. Tarascon, Nat. Mater. **4**, 367 (2005). https://doi.org/10.1038/nmat1368

3. S. R. Sivakkumar, J. M. Ko, D. Y. Kim, B. C. Kim, and G. G. Wallace, Electrochim. Acta **52**, 7378 (2007). https://doi.org/10.1016/j.electacta.2007.06.023
4. Z. Chen, Y. Qin, D. Weng, Q. Xiao, Y. Peng et al., Adv. Funct. Mater. **19**, 3421 (2009). https://doi.org/10.1002/adfm.200900971
5. H. Chen, X. Q. Qi, M. Kuang, F. Dong, and Y. X. Zhang, Electrochim. Acta **212**, 672 (2016). https://doi.org/10.1016/j.electacta.2016.07.024
6. J. -J. Ruan, Y.-Q. Huo, and B. Hu, Electrochim. Acta **215**, 109 (2016). https://doi.org/10.1016/j.electacta.2016.08.064
7. J. Xu, C. Ma, J. Cao, and Z. Chen, Dalton Trans. **46**, 3277 (2017). https://doi.org/10.1039/C6DT04759A
8. M. H. Priyadarsini, M. C. Jena P. Adhikary, and R. M. Pujahari, J. Sci. Res. **15**, 43 (2023). https://doi.org/10.3329/jsr.v15i1.59397
9. D. S. Dalavi, R. S. Desai, and P. S. Patil, J. Mater. Chem. A **10**, 1180 (2022). https://doi.org/10.1039/D1TA07237D
10. L. Lv, K. Xu, C. Wang, H. Wan, Y. Ruan et al., Electrochim. Acta **216**, 36 (2016). https://doi.org/10.1016/j.electacta.2016.08.149
11. J. Balamurugan, T. D. Thanh, S.-B. Heo, N. H. Kim, and J. H. Lee, Carbon **94**, 963 (2015). https://doi.org/10.1016/j.carbon.2015.07.087
12. Y. Zhao, X. Zhang, J. He, L. Zhang, M. Xia, and F. Gao, Electrochim. Acta **174**, 52 (2015). https://doi.org/10.1016/j.electacta.2015.05.162
13. Y. Zhang, J. Xu, Y. Zheng, Y. Zhang, X. Hu, and T. Xu, RSC Adv. **7**, 3984 (2017). https://doi.org/10.3390/nano7090273
14. S. K. Kaverlavani, S. E. Moosavifard, and A. Bakouei, Chem. Commun. **53**, 1053 (2017). https://doi.org/10.1016/j.jallcom.2019.02.134
15. L. Wang, M. Arif, G. Duan, S. Chen, and X. Liu, J. Power Sour. **355**, 54 (2017). https://doi.org/10.1016/j.jpowsour.2017.04.054
16. T. Wang, M. Liu, and H. Ma, Nanomaterials **7**, 140 (2017). https://doi.org/10.3390/nano7060140
17. S. S. Gaikwad, S. S. Gaikwad, and D. S. Sutrave, J. Sci. Res. Sci. Technol. **9**, 163 (2021).
18. D. Sutrave, S. Jogade, and S. Gothe, Int. J. Res. Appl. Sci. Eng. Technol. **4**, 4 (2016).
19. S. Sukumar, A. Rudrasenan, and D. P. Nambiar, ACS Omega **5**, 1041 (2020). https://doi.org/10.1021/acsomega.9b02857
20. G. R. Chodankar, S. A. Sawant, S. R. Gurav, and R. G. Sonkawade, J. Shivaji University: Sci. Technol. **50**, 38 (2024).
21. P. S. Joshi, S. M. Jogade, S. D. Gothe, and D. S. Sutrave, Asian J. Chem. **29**, 203 (2017). https://doi.org/10.14233/ajchem.2017.20378
22. J. Yin and J. Park, Int. J. Hydrogen Energy **39**, 16563 (2014). https://doi.org/10.1016/j.ijhydene.2014.04.202
23. S. K. Shinde, D. P. Dubal, G. S. Ghodake, D. Y. Kim, and V. J. Fulari, J. Electro Analyt. Chem. **732**, 80 (2014). http://dx.doi.org/10.1016/j.jelechem.2014.09.004
24. P. Jadhav, V. V. Shinde, and G. J. Navathe, Am. Institute of Phys. Conf. Proc. **1536**, 679 (2013). https://doi.org/10.1063/1.4810409
25. A. H. Zimmerman and P. K. Effa, J. Electrochem. Soc. **131**, 710 (1984). https://doi.org/10.1149/1.2115677
26. R. D. Armstrong and W. Hong, Electrochim. Acta **36**, 759 (1991). https://doi.org/10.1016/0013-4686(91)85271-8
27. H. Xiao, S. Yao, H. Liu, F. Qu, X. Zhang, and X. Wu, Progr. Nat. Sci.: Mater. Int. **26**, 271 (2016). https://doi.org/10.1016/j.pnsc.2016.05.007